Brain and Spine 4 (2024) 102842

Contents lists available at ScienceDirect

Brain and Spine

journal homepage: www.journals.elsevier.com/brain-and-spine

Unveiling the natural history of paralysis in metastatic cervical spinal tumor: An experimental study

Shunsuke Sato [a], Masahito Takahashi [a,*], Kazuhiko Satomi [b], Hideaki Ohne [a], Takumi Takeuchi [a], Atsushi Hasegawa [a], Shoichi Ichimura [c], Naobumi Hosogane [a]

[a] Department of Orthopaedic Surgery, Kyorin University, Tokyo, Japan
[b] Orthopaedic Surgery, Mitaka Hospital, Tokyo, Japan
[c] Orthopaedic Surgery, Kyorin University Suginami Hospital, Tokyo, Japan

ARTICLE INFO

Handling Editor: Prof F Kandziora

Keywords:
Cervical spine
Experimental study
Metastatic spinal tumor
Paralysis
Epidural tumor

ABSTRACT

Introduction: Despite the relatively low prevalence of metastatic cervical spinal tumor, these entities give rise to more profound complications than thoracic and lumbar spinal tumor. However, it is regrettable that experimental investigation has thus far shown a dearth of attention to metastatic cervical spinal tumor.
Research question: What is the conceptualization and realization of quadriparesis resulting from metastatic cervical spinal tumor?
Material and methods: Using Fischer 344 rats as the experimental cohort, this study orchestrated the engraftment of tumor cells procured from the 13762 MAT B III cell line (RRID: CVCL_3475), which represents mammary adenocarcinoma. These cells were engrafted into the vertebrae of the cervical spine. A comprehensive inquiry encompassing behavioral assessments, histological evaluations, and microangiographic analyses conducted after the aforementioned cellular transplantation was subsequently pursued.
Results: The incidence of cervical paralysis was 61.1%. Notably, the evolution of paralysis was unfurled by two distinctive temporal phases within its natural history. A meticulous histological examination facilitated delineation of the tumor's posterior expansion within the spinal canal. Simultaneously, the tumor exhibited anterior and lateral encroachment on the spinal cord, inducing compression from all sides. Augmented by microangiographic investigations, conspicuous attenuation of stained blood vessels within the affected anterior horn and funiculus of the spinal cord was observed.
Discussion and conclusion: The pathological advancement of paralysis stemming from metastatic cervical spinal tumor is now apprehended to unfurl through a biphasic phase. The initial phase is characterized by gradual unfurling spanning several days, juxtaposed against the second phase marked by swift and accelerated progression.

1. Introduction

Almost all types of systemic cancer can metastasize to the spinal column, and epidural spinal compression has been reported in every major type of systemic cancer (Prasad and Schiff, 2005). The thoracic spine (60%–80%) emerges as the foremost site of involvement, followed by the lumbar region (15%–30%), and the cervical spine (<10%) (Sutcliffe et al., 2013). However, notwithstanding the relatively lower prevalence of metastatic cervical spinal tumor (MCST), this entity causes more profound complications when juxtaposed with their thoracic and lumbar counterparts. Beyond its unique capacity to induce quadriplegia, MCST can also precipitate respiratory failure. Hence, MCST is associated with a less favorable prognosis than thoracic and lumbar metastases. Various clinical algorithms for the management of metastatic spinal tumors have been documented (Spratt et al., 2017a; Quraishi et al., 2010; Kaloostian et al., 2014; Barzilai et al., 2018; Paulino Pereira et al., 2016). The main candidate treatments are radiation, surgery, and chemotherapy; however, the timing of interventions for radiation and surgery has not been clarified using data from an experimental study.

Several experimental studies have been documented to enhance the management of metastatic spinal tumors. A significant proportion of these investigations focused on paraplegia resulting from thoracic or

* Corresponding author. Department of Orthopaedic Surgery, Kyorin University, 6-20-2 Shinkawa, Mitaka City, Tokyo, 181-8611, Japan.
E-mail address: mtaka@ks.kyorin-u.ac.jp (M. Takahashi).

https://doi.org/10.1016/j.bas.2024.102842
Received 18 January 2024; Received in revised form 23 April 2024; Accepted 24 May 2024
Available online 25 May 2024

lumbar metastases (Ushio et al., 1977; Kato et al., 1985; Siegal et al., 1987; Mantha et al., 2005; Amundson et al., 2005a). However, no experimental study has examined cervical paralysis in the context of MCST. Therefore, it is imperative to establish an animal model of MCST and systematically scrutinize the natural progression of cervical paralysis, thereby refining treatment algorithms.

This study delineates the methodology for creating a novel MCST model and comprehensively elucidates the ensuing natural history of cervical paralysis. Our findings can help to improve unsatisfactory results in the treatment of MCST.

2. Material and Methods

2.1. Animals

Fischer 344 female rats (n = 20; 180–220 g, 10 weeks old) were used as experimental cohorts. All experimental protocols were ethically sanctioned by the Committee for Animal Experimentation and rigorously adhered to the established guidelines stipulated by the Ministry of Education, Culture, Sports, Science, and Technology of the nation. The subjects were anesthetized by intraperitoneal injection of a mixture of 60 μg/g ketamine (Daiichi Sankyo Company, Tokyo, Japan) and 100 μg/g xylazine hydrochloride (Bayer Health Care, Monheim, Germany).

2.2. Experimental protocol (Fig. 1)

Eighteen rats underwent transplantation of tumor mass into the cervical vertebral body. Behavioral assessments were conducted subsequent to the transplantation. Following the onset of paralysis, histological examinations were performed at various intervals. Microangiography was conducted on two rats that developed paralysis. Rats that died prior to exhibiting paralysis were examined to determine the potential causes of death. In the two rats that underwent sham surgery.

2.3. Tumor cell line

The CRL-1666 mammary adenocarcinoma cell line (RRID: CVCL_3475, 13762 MAT B III) was selected for this experiment from the American Type Culture Collection (Manassas, VA, USA). To procure solid tumor samples from the cell line, carrier animals of the Fischer 344 strain received a subcutaneous injection of 106 CRL-1666 cells into the proximal hindlimb. Ten days post-injection, the animals were humanely euthanized using pentobarbital (120 mg/kg, intraperitoneal injection), followed by resection of the tumor, which was subsequently immersed in a 0.9% sterile NaCl solution. Tumor masses designated for transplantation were meticulously sectioned into dimensions of 1.5 × 1.5 × 1.5 mm (Mantha et al., 2005).

2.4. Surgical technique of tumor mass transplantation

Following intraperitoneal anesthesia, the anterior neck was depilated and treated with a scrub solution containing 7.5% ISODINE (Mundipharma K.K., Tokyo, Japan). An incision was made in the anterior neck, exposing the cervical vertebrae via an anterior approach. Employing a high-speed surgical drill with a diameter of 1 mm, a cavity was meticulously fashioned within the cervical vertebral body to accommodate transplantation of the tumor mass. The cavity, approximately 3 mm deep and 2 mm wide, featured an ostium 1 mm in diameter, ensuring the prevention of anterior displacement of the tumor mass. The keyhole in the anterior wall of the vertebral body, created for cavity formation, should be as small as feasible during tumor transplantation to minimize the risk of the transplanted tumor invading the retropharyngeal and/or retrotracheal spaces (Fig. 2). After transplantation of the tumor mass into the vertebral body cavity, closure of the incision was performed using 3-0 Vicryl sutures (Johnson and Johnson, NJ, USA). Following full recovery, the rats were returned to their respective cages after thorough observation.

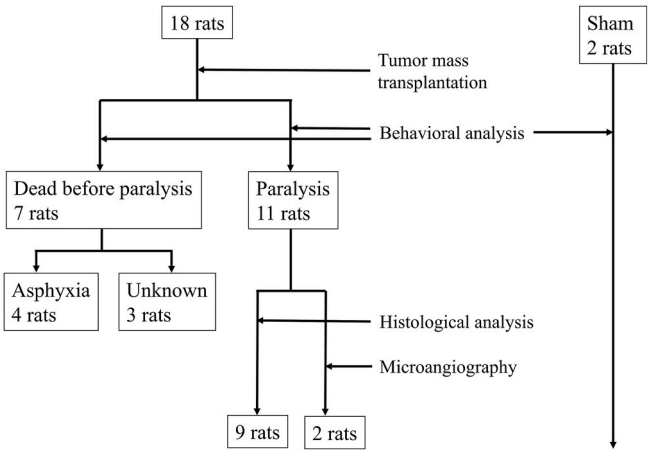

Fig. 1. Schema of the experimental protocol. Eighteen rats underwent transplantation of the tumor mass, while two rats received sham surgery. Eleven of the eighteen rats developed forelimb and/or hindlimb paralysis. Neither of the two rats that underwent sham surgery developed paralysis during the 30-day post-operative period, and both achieved full scores in behavioral analysis. The eleven rats that developed paralysis underwent behavioral assessments from days 1–20 post-transplantation. Depending on the progression of paralysis, these rats were euthanized for histological analysis. Microangiography was performed on two of these eleven rats to evaluate the vascular structures within the cervical spinal cord.

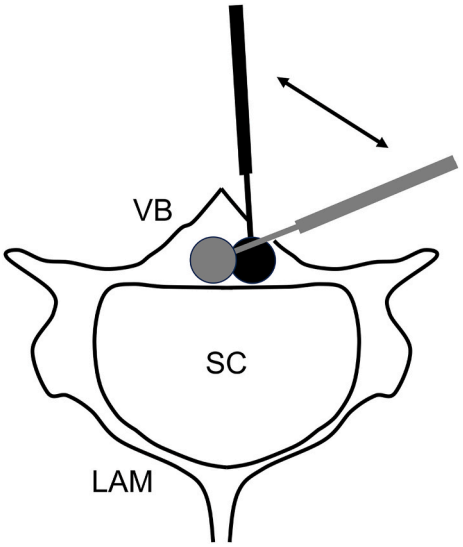

Fig. 2. Depiction of the Cervical Spine Cavity Creation Technique. A high-speed drill bar is employed to fashion a keyhole, subsequently creating a cavity suitable for the transplantation process. VB; vertebral body, SC; spinal canal, LAM; lamina.

The two rodents in the sham surgery underwent all standard procedures except for the transplantation of the tumor mass and were subsequently evaluated through behavioral analysis.

2.5. Behavioral analysis

The transplanted rats underwent an assessment of motor paralysis of both forelimbs and hindlimbs via open-field evaluation adapted for the evaluation of cervical spinal cord injury in rats (Martinez et al., 2009). Over a 2-week period, the rats were habituated to being handled

multiple times within the open field. Behavioral assessments were conducted on days 1, 7, 10, and 11–20 post transplantation. These evaluations were meticulously video-recorded and scored by a proficient orthopedic surgeon. Scoring was performed on two separate days, with the subsequent calculation of the mean scores for each behavioral assessment. Rigorous intra-rater reliability analysis and graphical assessments were conducted to ascertain the relationship between the post-transplantation time frames and the development of motor paralysis.

2.6. Histological analysis

In accordance with the outcomes of the behavioral analysis, transplanted rats that exhibited motor paralysis were humanely sacrificed to procure histological specimens from the transplanted spinal region. These specimens were subsequently subjected to hematoxylin and eosin staining at distinct time points corresponding to the onset and progression of paralysis.

2.7. Microangiography in the spinal cord

Under intraperitoneal anesthesia consisting of 60 μg/g ketamine (Daiichi Sankyo Company, Tokyo, Japan) and 100 μg/g xylazine hydrochloride (Bayer Health Care, Monheim, Germany), bilateral skin incisions were made in the inguinal area. The bilateral inguinal vessels were meticulously exposed, and a 0.5-mm-diameter cannula was used to cannulate the right inguinal vein. A perfusion protocol was implemented using a mixture of 250 ml of normal saline and 5000 U heparin, lasting 1–2 min. The left inguinal artery was incised to allow for blood drainage and verification of blood color. Upon attenuation of blood color, perfusion was promptly ceased and replaced with 100 ml of India ink infused with 10 g of liquid gelatin at a temperature of 40 °C (Erol et al., 1980). Following resection of the cervical spine, the specimens were immersed in 10% formalin for one week. After resection, the cervical spinal cord specimens were meticulously sectioned into 50 μm slices using a combination of the CLARITY and CUBIC protocols (FUJIFILM, Osaka, Japan) (Tomer et al., 2014).

3. Results

3.1. Behavioral analysis

Behavioral analysis revealed forelimb and/or hindlimb paralysis in 11 of the 18 transplanted rats (61.1%). All rats without paralysis that succumbed before the manifestation of paralysis were documented. Among these, four out of seven rats (57.1%) experienced asphyxia due to tumor-induced tracheal compression and subsequently died.

In terms of the forelimb behavioral score, the onset of paralysis varied between postoperative days 12 and 17. Rats #5, #7, #9, and #11 exhibited a rapid decline in forelimb behavioral scores within 2 days. Rats #2 and #6 experienced an abrupt decrease in scores upon the detection of forelimb palsy (Fig. 3A). Regarding hindlimb behavioral scores, the onset of paralysis ranged between 12 and 17 days postoperatively. Notably, the onset of paralysis was consistent between the forelimb and hindlimb. Among rats #5, #9, and #11, hindlimb behavioral scores gradually declined over 1–2 days, followed by a sharp decrease (Fig. 3B).

The mean forelimb behavioral score exhibited an initial decline commencing at day 14.5 ± 1.7 postoperatively, followed by a steep reduction around postoperative day 16. Similarly, the mean hindlimb behavioral score commenced diminishing at day 14.4 ± 1.5 postoperatively and experienced a steep decline around day 18 postoperatively. Notably, the progression of both forelimb and hindlimb paralysis was characterized by nonconstant, nonlinear deterioration rates. The natural course of paralysis development revealed two distinct phases: an initial gradual progression over a few days followed by a subsequent rapid exacerbation (Fig. 3C).

3.2. Histological analysis

Photomicrographs of the transplanted C5 vertebra in rat #7 (forelimb score; 9, hindlimb score; 17 on day 17) illustrate the development of the transplanted tumor within the vertebra, extending anteriorly toward the spinal canal. The tumor expanded posteriorly within the spinal canal, exerting compression on the spinal cord, as it encircled anteriorly and laterally. Notably, no tumor infiltration was observed within the

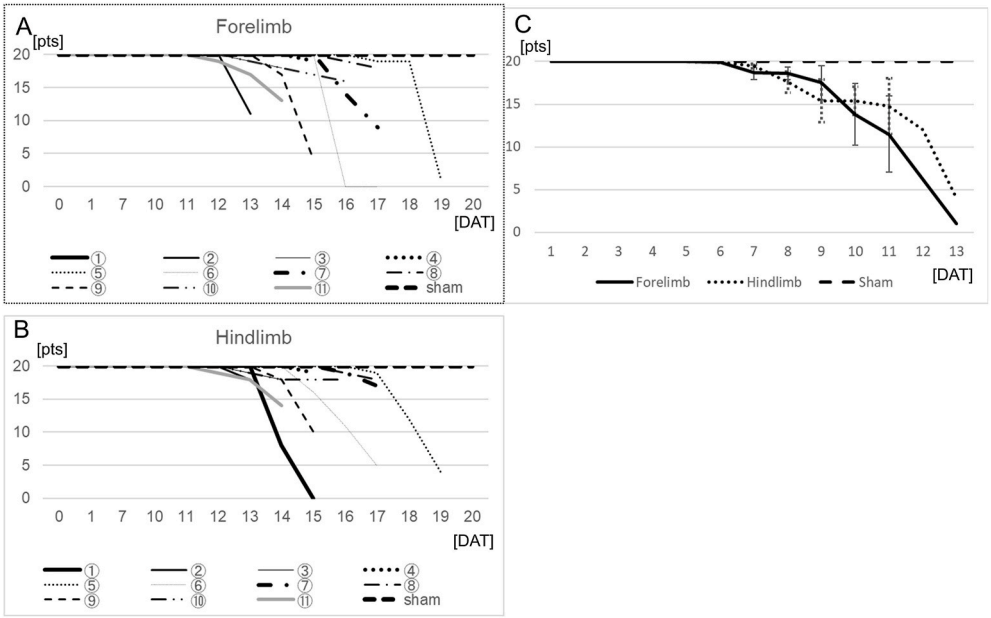

Fig. 3. Temporal Profile of the behavioral score. A: Forelimb behavioral scores for each transplanted rat. B: Hindlimb behavioral scores. C: Mean scores for forelimb and hindlimb assessments. The earliest onset of paralysis occurred on day 12 postoperatively for both forelimbs and hindlimbs. The mean score gradually declined until day 15 postoperatively for the forelimb and day 17 for the hindlimb, followed by rapid reduction. Error bars represent standard errors. pts: Points from the open-field evaluation, DAT: Days after transplantation.

intradural space (Fig. 4).

In instances of transplanted rats experiencing gradual paralysis development, such as rat #10 (forelimb score; 16, hindlimb score; 18 on day 16) and rat #8 (forelimb/hindlimb score; 18 on day 17), the tumor infiltrated the anterior and lateral spinal canals. The extent of invasion was confined to less than 25% of the anterior region of the spinal canal (Fig. 5A and B). Conversely, in the case of rat #6 (forelimb score; 0, hindlimb score; 5 on day 17) presenting with severe palsy, the tumor within the anterior spinal canal encroached upon approximately 50% of the spinal canal space, leading to a significant reduction in the axial dimensions of the spinal cord (Fig. 5C).

3.3. Microangiography

Microangiography performed on rat #4 (forelimb score; 19, hindlimb score; 19 on day 15) revealed diminished vascularity within the anterior funiculus on the more compressed side, along with a non-staining area in the anterior gray matter. Intrinsic arteries within the posterior half of the spinal cord were preserved (Fig. 6).

4. Discussion

In the existing literature on metastatic spinal tumors, there is a conspicuous absence of experimental studies addressing Metastatic Cervical Spinal Tumors (MCST). Prior research has primarily focused on establishing experimental models for metastasis within the thoracic and lumbar spinal regions (Spratt et al., 2017a; Amundson et al., 2005a, 2005b; Takahashi et al., 2004; Gok et al., 2009). Nevertheless, these models remain inherently limited as they fail to capture the natural progression of forelimb palsy, an analog of upper-extremity palsy in human contexts. The paucity of studies addressing MCST models could be attributed to the intricate procedures associated with transplanting a tumor mass into the confined space of the cervical spine. Constrained transplantation sites inevitably lead to challenges in terms of model replicability. Furthermore, transplanted tumors have the potential to encroach beyond the cervical spine, resulting in asphyxia via tracheal compression, ultimately leading to death. In a previous study, we reported a model involving metastatic lumbar spinal tumors causing hindlimb paralysis in rabbits with a repeatability rate of 60.0% (Takahashi et al., 2004). Similarly, Amundson et al. documented a repeatability rate of 72.0% in their experimental investigation of thoracic spinal tumors and paralysis in rabbits (Amundson et al., 2005b). Within our current model, the repeatability rate was 61.1%, which is deemed acceptable for an MCST model associated with paralysis.

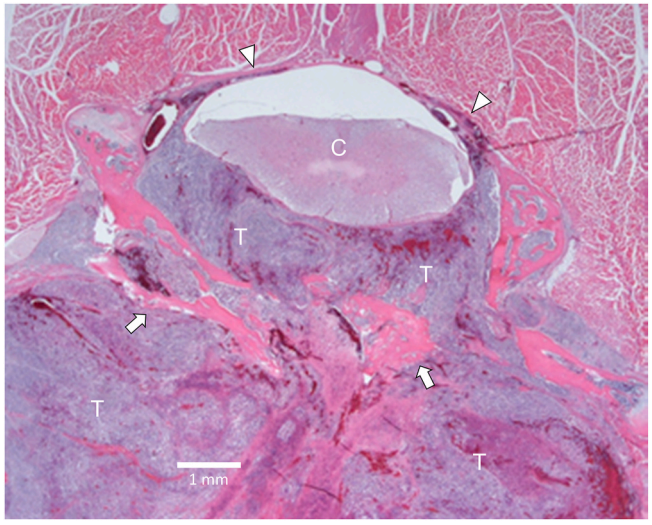

Fig. 4. Photomicrography of transplanted C5 vertebra of rat #7 (forelimb score: 9, hindlimb score: 17 at day 17 after transplantation). The transplanted tumor developed within the vertebra, invading from the anterior to lateral and posterior spinal canal. The tumor exerted compression on the spinal cord, both anteriorly and laterally. T: Tumor, C: Spinal cord, Arrow; Vertebral body, Arrowhead; Lamina.

Forelimb paralysis did not consistently precede hindlimb paralysis in the present study. As the transplanted tumor grew within the vertebral body, it progressively infiltrated the spinal canal, ultimately resulting in compression of the anterior spinal cord (Fig. 3A). Given that the ventral spinal artery (VSA) supplies blood to the ventral gray matter (Turnbull, 1973), compression of the VSA compromises the blood supply to the anterior spinal cord in accordance with the anatomical arrangement of the intrinsic spinal arteries. Consequently, forelimb paralysis is expected to precede hindlimb paralysis. However, our behavioral analysis, employing open-field evaluations for both forelimb and hindlimb paralysis, indicated an average onset of paralysis of approximately 14 days postoperatively. It is important to note that this evaluation might not possess the precision required to detect early onset forelimb paralysis. For a more accurate assessment of forelimb paralysis, it is recommended to employ an analysis such as the “reach and grasp task, as elucidated by Whishaw IQ et al. (Whishaw et al., 1998).

In our study, the natural progression of paralysis stemming from the MCST revealed two distinct phases. The initial phase entails gradual paralysis development over several days, followed by a subsequent phase characterized by rapid and pronounced paralysis intensification. This is the first study to delineate the natural course of paralysis arising from the MCST. Notably, the International Spine Oncology Consortium previously established an algorithm for the management of patients with metastatic spinal tumors (Spratt et al., 2017b). With this algorithm, surgical intervention has emerged as the preferred treatment modality. Patchell et al. emphasized the superiority of surgical intervention as a first-line approach for patients manifesting neurological deficits (Patchell et al., 2005). Based on the outcomes of our study, the timing of surgical intervention is of paramount significance, especially given that neurological deficits are likely to exhibit rapid progression during the second phase of the disease course.

Histological analysis illuminated the trajectory of the transplanted tumor growth originating within the vertebral body and subsequently invading beyond its confines. In a rabbit model, Takahashi et al. reported that a tumor transplanted into the lumbar vertebra circumferentially invaded the spinal canal (Takahashi et al., 2004). Upon entering the spinal canal, the infiltrating tumor elicited both anterior and lateral spinal cord compression. This contrasts with other degenerative spinal conditions such as cervical disc herniation and cervical spondylosis. Consequently, progressive paralysis frequently manifests in metastatic spinal tumors.

Early in the course of tumor transplantation, invasion primarily targets the anterior spinal canal. However, this invasion gradually extended beyond the anterior canal, incorporating a lateral expansion. This multifaceted invasion pattern precipitated the aggravated paralysis. Severe spinal cord compression in both the anterior and lateral directions contributes to the progression of paralysis. Notably, no tumor cell infiltration was observed in the intradural spaces. In concordance with this, Fujita et al. expounded upon the rarity of intradural spinal tumor invasion, attributing this phenomenon to the dura mater’s role as a barrier to tumor infiltration (Fujita et al., 1997).

Microangiography conducted on a rat displaying partial paralysis (forelimb score, 9; hindlimb score, 17 in the open-field test) revealed diminished vascularity within the anterior funiculus on the side, with more pronounced compression. In addition, a non-stained region was evident within the anterior gray matter. In contrast, intrinsic arteries within the posterior spinal cord were preserved. Consequently, while forelimb paralysis was distinctly evident, hindlimb paralysis exhibited a limited presentation. The intrinsic arterial network of the rat spinal cord comprises the peripheral and central systems. The central system,

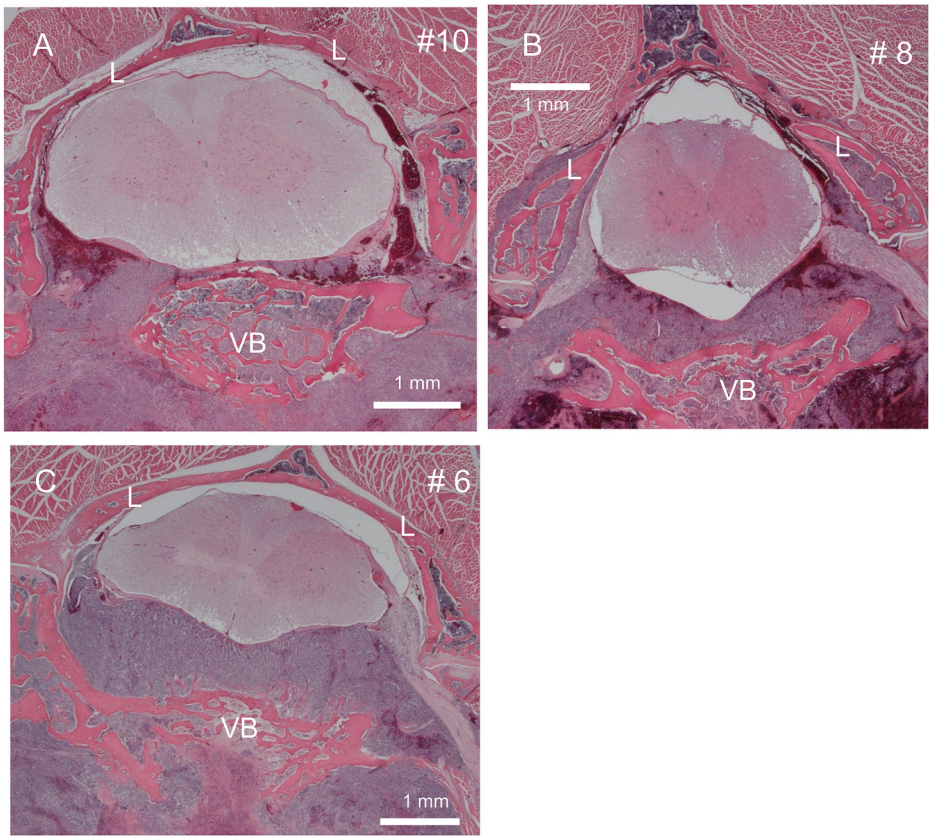

Fig. 5. Photomicrographs showing tumor invasion into the spinal canal from the vertebral body in conjunction with progressive paralysis. A: Rat #10 (forelimb score: 16, hindlimb score: 18 in the open-field test at day 16 postoperatively). B: Rat #8, (forelimb score: 18, hindlimb score: 18 at day 17 postoperatively). C: Rat #6, (forelimb score: 0, hindlimb score: 5 at day 17 postoperatively). VB: Vertebral body, L: Lamina. Hematoxylin and eosin staining was employed.

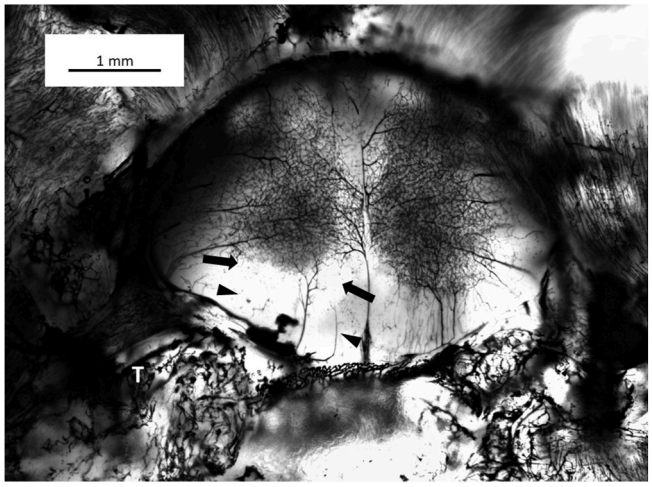

Fig. 6. Microangiography in rat #4 (Open-field test: forelimb score; 19, hindlimb score: 19 on day 15). Remarkable reduction in vascularity observed in the anterior funiculus (arrowheads) and the anterior horn (arrows) on the more compressed side of the spinal cord. T: Tumor.

originating from the VSA, perfuses the ventral two-thirds of the spinal cord (Mazensky et al., 2017). In theory, forelimb paralysis should precede hindlimb paralysis; however, in our study, the onset of paralysis was concurrent in both limb types. To achieve a more precise assessment of early forelimb paralysis, specialized behavioral testing dedicated solely to forelimb movement, such as the “reach and grasp task, " as described by Whishaw IQ et al. (Whishaw et al., 1998).

The pathogenesis of paralysis within this context stems from the dual interplay of mechanical compression of the spinal cord and circulatory disturbances in the intrinsic spinal arteries. Fig. 4 illustrates the progressive infiltration of the tumor within the vertebral body and into the spinal canal, mirroring the evolving paralysis. Additionally, Fig. 6 underscores the reduced arterial supply to the anterior funiculus and horn of the spinal cord in a paralyzed rat, correlating with the compressive effect of the tumor. Prior investigations by Kato et al. postulated that mechanical compression could lead to circulatory disruption within the spinal cord, potentially resulting in irreversible paralysis, and that spinal cord blood flow precipitously declines to critical levels (Kato et al., 1985). In our model, microangiography performed on a rat with incipient paralysis demonstrated reduced blood vessel density in the anterior funiculus and the anterior horn, despite minimal mechanical compression of the spinal cord. This suggests that the acceleration of paralysis in later stages may be predominantly due to a reduction in spinal cord blood flow.

Clinically, one of the pivotal considerations is the optimal timing of surgical intervention for patients experiencing paralysis due to metastatic spinal tumors. It is well-experienced that patients with mild paralysis can deteriorate rapidly, as spinal cord blood flow swiftly declines to critical levels. Therefore, it is imperative for spine surgeons to act expeditiously, particularly in cases where surgical intervention is indicated, to preclude further progression of paralysis. This biphasic natural course, marked by initial mild symptoms rapidly escalating to severe impairment, underscores the urgency of timely medical response.

This study had three potential limitations that merit consideration. Firstly, metastasis within our model did not mirror natural dissemination via blood flow. Vascular pathways and blood flow significantly influence metastatic patterns in cancer (Coleman, 2001). In our preliminary study, tumor cells were introduced via the femoral vein;

however, all rats succumbed to either tumor embolism or systemic metastasis. Consequently, the tumor mass was artificially implanted into the vertebral body. Secondly, subsequent paralysis progression within rats could not be evaluated after histological analysis. While histological analysis is a more accurate modality than imaging techniques such as computed tomography and magnetic resonance imaging, inherent limitations persist in this regard. Thirdly, the sample size of rodents used in the study posed a limitation. A more comprehensive evaluation of the initial stage of paralysis was necessary, particularly involving microangiography. The fragile tissue of the spinal cord complicates such analysis; once the spinal cord sustains severe damage, subsequent evaluation through microangiography becomes unfeasible. Acknowledging that rodents in the early stages of paralysis are more conducive for microangiographic analysis, incorporating a greater number of angiographic assessments during this phase would significantly strengthen the robustness of our research.

5. Conclusions

To elucidate the natural history of paralysis stemming from cervical spinal tumors, we successfully formulated an animal model. Within this model, the initial phase unfolds as a gradual progression over a span of several days, whereas the subsequent phase unfolds as rapid and intensified advancement.

Declaration of competing interest

This research did not receive any specific grant from funding agencies in the public, commercial, or not-for-profit sectors. All authors certify that they have no affiliations with or involvement in any organization or entity with any financial interest or non-financial interest in the subject matter or materials discussed in this manuscript.

Acknowledgments

The authors would like to acknowledge Ms. Mizuho Kosuge for her technical support.

References

Amundson, E., Pradilla, G., Brastianos, P., Bagley, C., Riley, L.H., Garonzik, I.M., McCarthy, E., Wolinsky, J.P., Gokaslan, Z.L., 2005a. A novel intravertebral tumor model in rabbits. Neurosurgery 57, 341–346. https://doi.org/10.1227/01.neu.0000166683.67906.b7.

Amundson, E., Pradilla, G., Brastianos, P., Bagley, C., RileyIM 3rd, L.H., Garonzik, McCarthy, E., Wolinsky, J.P., Gokaslan, Z., 2005b. A novel intravertebral tumor model in rabbits. Neurosurgery 57, 341–346. https://doi.org/10.1227/01.neu.0000166683.67906.b7.

Barzilai, O., Fisher, C.G., Bilsky, M.H., 2018. State of the art treatment of spinal metastatic Disease. Neurosurgery 82, 757–769. https://doi.org/10.1093/neuros/nyx567.

Coleman, R.E., 2001. Metastatic bone disease: clinical features, pathophysiology and treatment strategies. Cancer Treat Rev. 27, 165–176. https://doi.org/10.1053/ctrv.2000.0210.

Erol, O.O., Spira, M., Levy, B., 1980. Microangiography: a detailed technique of perfusion. J. Surg. Res. 29, 406–413. https://doi.org/10.1016/0022-4804(80)90053-0.

Fujita, T., Ueda, Y., Kawahara, N., Baba, H., Tomita, K., 1997. Local spread of metastatic vertebral tumors. A histologic study. Spine 22, 1905–1912. https://doi.org/10.1097/00007632-199708150-00020.

Gok, B., McGirt, M.J., Sciubba, D.M., Garces-Ambrossi, G., Nelson, C., Noggle, J., Bydon, A., Witham, T.F., Wolinsky, J.P., Gokaslan, Z.L., 2009. Adjuvant treatment with locally delivered OncoGel delays the onset of paresis after surgical resection of experimental spinal column metastasis. Neurosurgery 65, 193–199. https://doi.org/10.1227/01.NEU.0000345948.54008.82.

Kaloostian, P.E., Yurter, A., Zadnik, P.L., Sciubba, D.M., Gokaslan, Z.L., 2014. Current paradigms for metastatic spinal disease: an evidence-based review. Ann. Surg Oncol. 21, 248–262. https://doi.org/10.1245/s10434-013-3324-8.

Kato, A., Ushio, Y., Hayakawa, T., Yamada, K., Ikeda, H., Mogami, H., 1985. Circulatory disturbance of the spinal cord with epidural neoplasm in rats. J. Neurosurg. 63, 260–265. https://doi.org/10.3171/jns.1985.63.2.0260.

Mantha, A., Legnani, F.G., Bagley, C.A., Gallia, G.L., Garonzik, I., Pradilla, G., Amundson, E., Tyler, B.M., Brem, H., Gokaslan, Z.L., 2005. A novel rat model for the study of intraosseous metastatic spine cancer. J. Neurosurg. Spine 2, 303–307. https://doi.org/10.3171/spi.2005.2.3.0303.

Martinez, M., Brezun, J.M., Bonnier, L., Xerri, C., 2009. A new rating scale for open-field evaluation of behavioral recovery after cervical spinal cord injury in rats. J. Neurotrauma 26, 1043–1053. https://doi.org/10.1089/neu.2008.0717.

Mazensky, D., Flesarova, S., Sulla, I., 2017. Arterial blood supply to the spinal cord in animal models of spinal cord injury. A review. Anat. Rec. 300, 2091–2106. https://doi.org/10.1002/ar.23694.

Patchell, R.A., Tibbs, P.A., Regine, W.F., Payne, R., Saris, S., Kryscio, R.J., Mohiuddin, M., Young, B., 2005. Direct decompressive surgical resection in the treatment of spinal cord compression caused by metastatic cancer: a randomised trial. Lancet 366, 643–648. https://doi.org/10.1016/S0140-6736(05)66954-1.

Paulino Pereira, N.R., Janssen, S.J., van Dijk, E., Harris, M.B., Hornicek, F.J., Ferrone, M. L., Schwab, J.H., 2016. Development of a prognostic survival algorithm for patients with metastatic spine disease. J. Bone Joint Surg. Am. 98, 1767–1776. https://doi.org/10.2106/JBJS.15.00975.

Prasad, D., Schiff, D., 2005. Malignant spinal-cord compression. Lancet Oncol. 6, 15–24. https://doi.org/10.1016/S1470-2045(04)01709-7.

Quraishi, N.A., Gokaslan, Z.L., Boriani, S., 2010. The surgical management of metastatic epidural compression of the spinal cord. J. Bone Joint Surg. Br. 92, 1054–1060. https://doi.org/10.1302/0301-620X.92B8.22296.

Siegal, T., Siegal, T.Z., Sandbank, U., Shohami, E., Shapira, J., Gomori, J.M., Ben-David, E., Catane, R., 1987. Experimental neoplastic spinal cord compression: evoked potentials, edema, prostaglandins, and light and electron microscopy. Spine 12, 440–448. https://doi.org/10.1097/00007632-198706000-00004.

Spratt, D.E., Beeler, W.H., de Moraes, F.Y., Rhines, L.D., Gemmete, J.J., Chaudhary, N., Shultz, D.B., 2017a. An integrated multidisciplinary algorithm for the management of spinal metastases: an International Spine Oncology Consortium report. Lancet Oncol. 18, e720–e730. https://doi.org/10.1016/S1470-2045(17)30612-5.

Spratt, D.E., Beeler, W.H., de Moraes, F.Y., Rhines, L.D., Gemmete, J.J., Chaudhary, N., Shultz, D.B., Smith, S.R., Berlin, A., Dahele, M., 2017b. An integrated multidisciplinary algorithm for the management of spinal metastases: an International Spine Oncology Consortium report. Lancet Oncol. 18, e720–e730. https://doi.org/10.1016/S1470-2045(17)30612-5.

Sutcliffe, P., Connock, M., Shyangdan, D., Court, R., Ngianga-Bakwin, K., Clarke, A., 2013. A systematic review of evidence on malignant spinal metastases: natural history and technologies for identifying patients at high risk of vertebral fracture and spinal cord compression. Health Technol. Assess. 17, 1–274. https://doi.org/10.3310/hta17420.

Takahashi, M., Ogawa, J., Kinoshita, Y., Takakura, M., Mochizuki, K., Satomi, K., 2004. Experimental study of paraplegia caused by spinal tumors: an animal model of spinal tumors created by transplantation of VX2 carcinoma. Spine J. 4, 675–680. https://doi.org/10.1016/j.spinee.2004.06.006.

Tomer, R., Ye, L., Hsueh, B., Deisseroth, K., 2014. Advanced CLARITY for rapid and high-resolution imaging of intact tissues. Nat. Protoc. 9, 1682–1697. https://doi.org/10.1038/nprot.2014.123.

Turnbull, I.M., 1973. Chapter 5. Blood supply of the spinal cord: normal and pathological considerations. Clin. Neurosurg. 20, 56–84. https://doi.org/10.1093/neurosurgery/20.cn_suppl_1.56.

Ushio, Y., Posner, R., Kim, J.H., Shapiro, W.R., Posner, J.B., 1977. Treatment of experimental spinal cord compression caused by extradural neoplasms. J. Neurosurg. 47, 380–390. https://doi.org/10.3171/jns.1977.47.3.0380.

Whishaw, I.Q., Gorny, B., Sarna, J., 1998. Paw and limb use in skilled and spontaneous reaching after pyramidal tract, red nucleus and combined lesions in the rat: behavioral and anatomical dissociations. Behav. Brain Res. 93, 167–183. https://doi.org/10.1016/s0166-4328(97)00152-6.